Original Article

Quantitative apparent diffusion coefficient metrics for MRI-only suspicious breast lesions: any added clinical value?

Xue Li[1,2]^, Hong Wang[1,2], Jiayin Gao[1,2], Lei Jiang[1,2], Min Chen[1,2]

[1]Department of Radiology, Beijing Hospital, National Center of Gerontology, Institute of Geriatric Medicine, Chinese Academy of Medical Sciences, Beijing, China; [2]Graduate School of Peking Union Medical College, Chinese Academy of Medical Sciences, Beijing, China

Contributions: (I) Conception and design: M Chen, X Li, L Jiang; (II) Administrative support: M Chen, L Jiang; (III) Provision of study materials or patients: H Wang, J Gao, L Jiang, M Chen; (IV) Collection and assembly of data: X Li, J Gao, L Jiang; (V) Data analysis and interpretation: X Li, L Jiang; (VI) Manuscript writing: All authors; (VII) Final approval of manuscript: All authors.

Correspondence to: Lei Jiang, MD; Min Chen, MD. Department of Radiology, Beijing Hospital, National Center of Gerontology, Institute of Geriatric Medicine, Chinese Academy of Medical Sciences, No. 1 Dahua Road, Dongdan, Beijing 100730, China; Graduate School of Peking Union Medical College, Chinese Academy of Medical Sciences, Beijing, China. Email: jiang_belinder@sina.com; cjr.chenmin@vip.163.com.

Background: Suspicious breast lesions [Breast Imaging Reporting and Data System (BI-RADS) category 4 or 5] detected only by magnetic resonance imaging (MRI) and invisible on other initial imaging modalities (MRI-only lesions) are usually small and poorly characterized in previous literature, thus making diagnosis and management difficult. This study aimed to investigate the clinical significance of quantitative apparent diffusion coefficient (ADC) metrics derived from conventional diffusion-weighted imaging (DWI) on evaluating MRI-only lesions.

Methods: A total of 90 suspicious MRI-only lesions were evaluated, including 51 malignant and 39 benign lesions. Morphological and kinetic characteristics of all lesions (termed BI-RADS parameters) were described according to the BI-RADS lexicon on dynamic contrast-enhanced (DCE) imaging. Minimum, maximum, and mean ADC values (ADC_{min}, ADC_{max}, ADC_{mean}) were obtained by measuring the ADC map of DWI. $ADC_{heterogeneity}$ was then obtained by the following formula: $ADC_{heterogeneity} = (ADC_{max} - ADC_{min})/ADC_{mean}$. Diagnostic performance of these parameters was assessed and compared using the receiver operating characteristic (ROC) curve.

Results: Of the 90 MRI-only lesions, there were 45 masses and 45 non-mass lesions. Among BI-RADS parameters, only two different kinetic patterns were significantly different between benign and malignant groups (P=0.005 and P<0.001, respectively). The area under the ROC curve (AUC) of combined significant ADC parameters (ADC_{min}, ADC_{mean}, and ADC_{max}, all P≤0.001) was significantly higher than that of the two different kinetic patterns (P=0.006 for both). For MRI-only masses, only ADC_{mean} and ADC_{max}, among all BI-RADS and ADC parameters, had diagnostic value (combined AUC =0.833). For non-mass lesions, size, distribution, ADC_{min}, and ADC_{mean} were significantly different between benign and malignant groups (P=0.004, P<0.001, P=0.001, and P<0.001, respectively). In addition, ADC_{mean} had the highest diagnostic performance among all ADC parameters, regardless of mass or non-mass (AUC =0.825 and 0.812, respectively). $ADC_{heterogeneity}$ showed no significant differences, no matter in mass or non-mass groups (P=0.62 and 0.43, respectively).

Conclusions: In differentiating MRI-only suspicious lesions, quantitative ADC metrics generally performed better than BI-RADS parameters, and ADC_{mean} is still the best ADC parameter to distinguish MRI-only lesions.

^ ORCID: 0000-0003-1759-2316.

Keywords: Diffusion-weighted imaging (DWI); apparent diffusion coefficient (ADC); magnetic resonance imaging (MRI); breast lesions

Submitted Mar 15, 2023. Accepted for publication Aug 25, 2023. Published online Sep 12, 2023.
doi: 10.21037/qims-23-331
View this article at: https://dx.doi.org/10.21037/qims-23-331

Introduction

Breast magnetic resonance imaging (MRI), as a functional imaging technique, shows the highest sensitivity (96%) for detecting breast cancer and has become an indispensable imaging modality for detecting breast lesions (1). Consequently, breast MRI can detect suspicious breast lesions yet undetected by mammography and ultrasound. Breast Imaging Reporting and Data System (BI-RADS), proposed by the American College of Radiology (ACR) (2), has been widely used in breast MRI. It applies categories 0 to 6 for the final assessment and breast lesions designated as suspicious for cancer (i.e., BI-RADS category 4 or 5) require further pathologic examination. Herein, we defined breast lesions of category 4 or 5, visible on breast MRI but not detected by initial mammography and ultrasound, as "MRI-only" breast lesions.

Such lesions are often small, poorly characterized in literature and lack typical morphologic features, making decision-making and clinical management difficult. Second-look ultrasound (SLU) is primarily suggested for their biopsy. However, the detection rate of SLU is variable, ranging from 50.7% to 69% (3-5), due to differences in physician experience and equipment limitation. Therefore, MRI-guided vacuum-assisted breast biopsy (VABB) was required for histological verification for lesions undetected by SLU. Although magnetic resonance (MR)-guided VABB is a valuable and safe technique (6), it presents a range of issues. MRI-compatible biopsy system is relatively expensive and not readily available. Furthermore, operation of breast MRI-guided biopsy is complex and time-consuming, requiring high expertise of the operator. The positive predictive value (PPV) of MRI-guided biopsy is less than 50% (7). This suggests that almost half the patients received unnecessary invasive biopsies for MRI-only lesions. Therefore, non-invasively and precisely diagnosing MRI-only lesion to avoid unnecessary biopsy is of great clinical significance.

Diffusion-weighted imaging (DWI), as a non-invasive non-enhanced MRI technique, has been increasingly incorporated into conventional MRI protocols (8). Apparent diffusion coefficient (ADC) derived from DWI can quantitatively analyze water diffusion in the microenvironment of breast tumors (8). Lots of previous studies confirmed its value in detection, differentiation, prognosis and efficacy evaluation of breast lesions (9-11). However, few studies (12,13) investigated DWI sequences in diagnosing MRI-only lesions. Spick *et al.* (12) evaluated the role of DWI in MRI-only breast lesions and found that additional application of DWI in MRI-only lesions could prevent false positives and reduce unnecessary biopsies. In recent years, some scholars noticed the role of quantitative ADC metrics on breast lesion differentiation. Texture and radiomic analysis based on ADC maps can quantitatively differentiate benign from malignant tumors and have been demonstrated to provide information about the heterogeneous biology of breast cancer but are limited by technical standardization and complex, time-consuming postprocessing (14,15). Consequently, a more direct and general method for clinical use is warranted. Kim *et al.* (16) proposed a quantitative assessment of heterogeneity in ADC values (i.e., ADC_{min}, ADC_{max}, ADC_{mean}, and $ADC_{heterogeneity}$) and stated that these metrics could provide biological clues to molecular subtypes of breast cancer. Can the straightforward method of measuring $ADC_{heterogeneity}$ have some added value for further discriminating MRI-only breast lesions? Therefore, in our current work, we quantitatively assessed the heterogeneity of ADC values in addition to ADC_{mean}, aiming to further explore the diagnostic value of conventional DWI sequences for MRI-only lesions. We present this article in accordance with the STARD reporting checklist (available at https://qims.amegroups.com/article/view/10.21037/qims-23-331/rc).

Methods

Study population

This retrospective study was conducted in accordance with the Declaration of Helsinki (as revised in 2013) and

Table 1 DWI and DCE protocol

Parameters	DWI	DCE
Sequence	Single-shot spin-echo-echo-planar imaging	Three-dimensional fast spoiled gradient echo
TR (ms)	7,000	5/7.08
TE (ms)	60	3/3.56
Flip angle (°)	90	10
FOV (mm^2)	340×340	320×320/340×340
Matrix	160×96	384×256
Voxel size (mm^3)	2.1×3.5×3.0	0.8×1.3×2.0/0.9×1.3×2.0
ST (mm)	3.0	2.0
No. of sections	48	96
Fat suppression	Frequency selection saturation	Spectral selected attenuated inversion recovery
Phases	NA	1 pre-contrast and 7 post-contrast
b values (s/mm^2)	50, 1,000	NA
Averages	2 (b=50), 7 (b=1,000)	NA
Diffusion mode	3-scan trace	NA

DWI, diffusion-weighted imaging; DCE, dynamic contrast-enhanced; TR, repetition time; TE, echo time; FOV, field of view; ST, section thickness; NA, non-applicable.

was approved by the Institutional Review Board of Beijing Hospital (No. 2022BJYYEC-388-01). The requirement for written informed consent was waived due to the retrospective nature of the study. Between January 2018 and December 2021, 1,485 female patients who underwent breast MRI at our hospital were enrolled. The inclusion criteria for this study were: (I) breast lesions evaluated as BI-RADS category 4 or 5 on MRI and confirmed pathologically; (II) imaging and pathology data are complete and available; and (III) negative initial mammographic and ultrasound findings. A total of 99 patients with 112 lesions were included in the study. We excluded the following patients: (I) who were biopsied or treated before MRI examination (n=6); (II) who lacked DWI sequence in the scan protocol (n=2) or whose lesions were invisible on DWI (n=10). Finally, a total of 81 patients with 90 lesions were included in the study.

MRI acquisition

MRI breast examinations were performed on 3.0T MRI (Discovery 750; GE Medical Systems, GE HealthCare, Anaheim, CA, USA) using a dedicated 8-channel phased-array breast coil. MRI studies used state-of-the-art breast MRI acquisition protocol, including fat-suppressed T2-weighted fast spin-echo sequence, DWI with ADC maps and fat-suppressed T1-weighted sequences before and after intravenous gadolinium-based contrast agents for dynamic contrast-enhanced (DCE) imaging with an injection rate of 2.5 mL/s (*Table 1*).

MRI interpretation and measurements

All cases were randomized and were reviewed on the MRI postprocessing workstation (AW4.6, GE HealthCare) by two radiologists (with 10 and 15 years of experience in breast MRI diagnosis, respectively) who independently interpreted the MRI characteristics of MRI-only lesions and were blinded to the clinical and pathological information. In case of disagreement, discussion between the two readers was performed to reach a consensus.

DCE evaluation

According to the 2013 version of BI-RADS MRI lexicon, the following morphological features were evaluated: for masses, size (the longest diameter), shape (oval or round/irregular), margin (circumscribed/not circumscribed), and internal enhancement (homogeneous/heterogeneous or rim

enhancement); for non-mass enhanced lesions, distribution (focal/others) and internal enhancement (homogeneous/heterogeneous or others).

Kinetic features of all lesions were assessed by time-intensity curve (TIC). TIC was generated from dynamic series using Functool Software (AW4.6, GE HealthCare) and was categorized into three types: plateau, persistent, and washout. The two radiologists manually and independently drew a region of interest (ROI) between 2 and 4 mm^2 on the brightest enhanced area, avoiding bleeding and necrotic regions.

The above morphological and kinetic characteristics were termed BI-RADS parameters.

DWI analysis

ADC maps were generated from DWI. Using T2-weighted imaging and DCE images as reference, the radiologists visually identified hyperintensity on DWI images with high b-value corresponding to the enhancing lesions on DCE. Subsequently, two-dimensional (2D) ROIs were manually delineated around the tumor contours at the slice of largest cross-sectional area of the lesion on ADC maps while avoiding bleeding, necrosis, cystic areas and tumor margin. ADC values for each ROI were calculated based on pixels. Finally, the minimum, mean, and maximum ADC values from each ROI were recorded as ADC_{min}, ADC_{mean}, and ADC_{max}. $ADC_{heterogeneity}$ was calculated using the formula (16):

$$ADC_{heterogeneity} = \left(ADC_{max} - ADC_{min}\right) / ADC_{mean} \quad [1]$$

Hereafter, ADC_{min}, ADC_{mean}, ADC_{max}, and $ADC_{heterogeneity}$ were generally called ADC parameters.

Reference standard

For these 90 MRI-only lesions, SLU was subsequently performed. If SLU failed to detect the lesion, open surgery directed by the lesion location and depth on MRI was performed to obtain and remove the pathologic tissue. Intraoperative fast frozen pathology was applied for tissue confirmation. For patients with nipple discharge, methylene blue dye was injected into lactiferous duct through nipple to assist surgery during operation.

Two experienced pathologists evaluated the pathological specimens in consensus. According to pathological findings, the lesions were divided into two groups: benign and malignant.

Statistical analysis

All statistical analyses were performed using IBM SPSS version 26 (IBM, Chicago, IL, USA) and MedCalc version 15.6.1 (MedCalc Software bvba, Ostend, Belgium). A P value <0.05 (two-tailed) was considered statistically significant. Correction for multiple comparisons was performed using a Bonferroni correction, and P values <0.0042 adjusted with the Bonferroni method were considered significantly different.

Continuous variables were presented as means ± standard deviations, while categorical variables were presented as frequency. Univariate analysis was performed using the chi-square test or Fisher's exact test to compare qualitative variables between benign and malignant lesions. For comparing quantitative variables, Kolmogorov-Smirnov test was used to evaluate the normality of distribution, and the Student's *t*-test or Mann-Whitney *U* test was applied to assess statistical differences between the two pathological groups. Based on the significant qualitative or quantitative variables identified by univariate analysis, receiver operating characteristic (ROC) curves were generated using logistic regression models to obtain the area under the ROC curve (AUC) and, furthermore, the sensitivity and specificity at the best cut-off point were determined by identifying the maximum Youden's index.

Results

Basic characteristics of patients and breast lesions

Patient selection protocol is presented in *Figure 1*. The age of patients was 50.9±11.0 (range, 29–72) years, and the size of lesions was 17.5±16.4 (range, 4–77) mm. Methods of obtaining pathology include SLU-guided biopsy (n=37), MRI-directed surgery (n=50), and methylene blue-assisted surgery (n=3). Nine patients had two lesions, of whom four had two benign lesions in the ipsilateral breast, two had two malignant lesions in ipsilateral breast, two had one benign lesion in each breast, and one had a benign lesion in one breast and a malignant lesion in the other.

Table 2 presents the histopathologic information of MRI-only breast lesions. Two representative cases of MRI-only lesions are shown in *Figures 2*,*3*.

BI-RADS parameters of MRI-only lesions

Table 3 shows the results of univariate analysis of all BI-

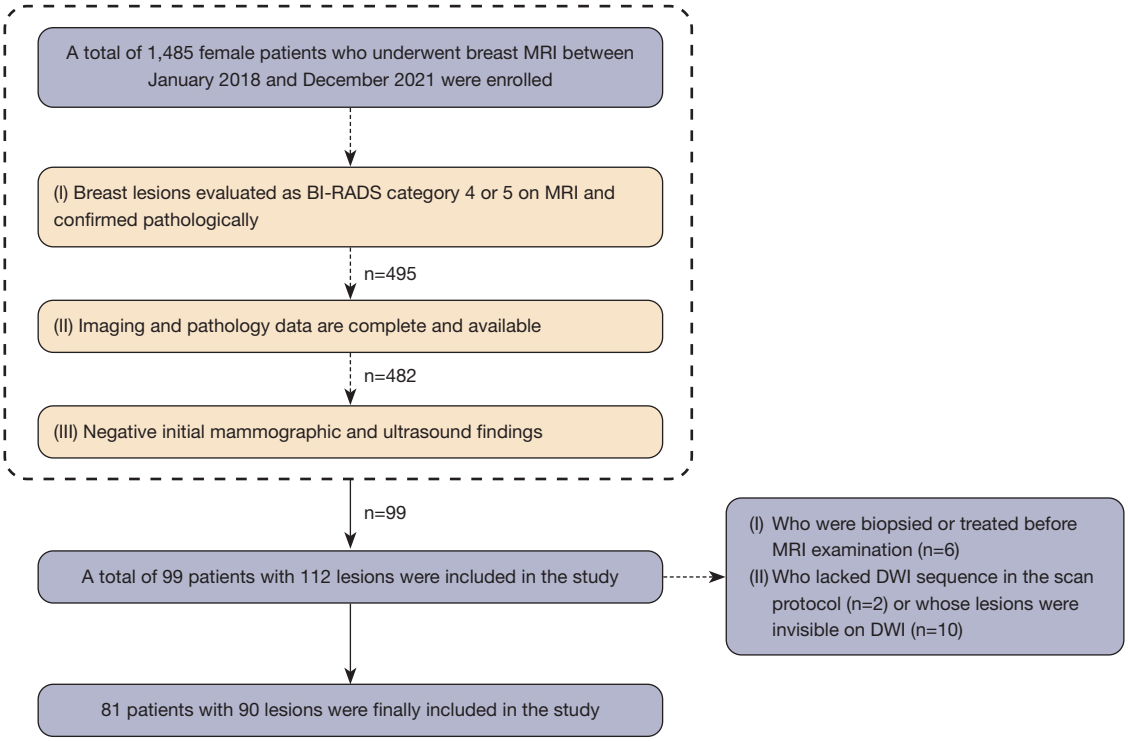

Figure 1 Flow diagram of patient selection process. MRI, magnetic resonance imaging; BI-RADS, Breast Imaging Reporting and Data System; DWI, diffusion-weighted imaging.

RADS parameters.

For all lesions, there was no significant difference in tumor size between benign and malignant lesions (14.8±14.2 *vs.* 19.6±17.8 mm, P=0.16). When washout pattern was defined as malignancy, there was significant difference in kinetic pattern between benign and malignant lesions (P=0.005) with AUC of 0.650 [95% confidence interval (CI): 0.542, 0.748], sensitivity of 60.78%, specificity of 69.23%, PPV of 0.721, and negative predictive value (NPV) of 0.574. When washout or plateau patterns were defined as malignancy, there was significant difference in kinetic pattern between benign and malignant groups (P<0.001), resulting in AUC, sensitivity, specificity, PPV, and NPV of 0.673 (95% CI: 0.566, 0.768), 96.08%, 38.46%, 0.671, and 0.882, respectively.

In mass lesions, our results revealed that MRI findings of mean size, shape, margin, and internal enhancement were not significantly different between benign and malignant lesions (P=0.07–0.85).

In non-mass lesions, there was significant difference in distribution between benign and malignant lesions (P<0.001), resulting in AUC of 0.620 (95% CI: 0.464, 0.761), sensitivity of 74.07%, specificity of 50.00%, PPV of 0.690, and NPV of 0.562. The mean sizes between benign and malignant non-mass lesions had significant difference (23.5±17.3 *vs.* 30.4±18.6 mm, P=0.004) with AUC, sensitivity, specificity, PPV, and NPV of 0.738 (95% CI: 0.585, 0.857), 70.37%, 77.78%, 0.676, and 0.636, respectively. Combining tumor size and distribution, a BI-RADS model was generated, in which AUC was 0.745 (95% CI: 0.593, 0.863) with sensitivity, specificity, PPV, and NPV of 62.96%, 88.89%, 0.769, and 0.632, respectively.

ADC parameters of MRI-only lesions

Table 4 presents the univariate analysis of ADC parameters for MRI-only lesions. *Table 5* demonstrates the results of ROC analysis.

Overall, ADC_{mean} performed best among all ADC parameters, regardless of mass or non-mass, with AUCs ranging from 0.809 to 0.825.

For all lesions, malignant lesions had significantly lower

Table 2 Histopathologic information of MRI-only breast lesions

Variables	Frequency	Percentage (%)
Pathology-obtaining method		
SLU guided biopsy	37	41.11
MRI-directed surgery	50	55.56
Methylene blue assisted surgery	3	3.33
Benign	39	43.33
Fibroadenoma	3	3.33
Papilloma	12	13.33
Adenosis	10	11.11
Usual/atypical ductal hyperplasia	9	10.00
Others	5	5.56
Malignant	51	56.67
Ductal carcinoma in situ	16	17.78
IDC	19	21.11
IDC with ductal carcinoma *in situ*	10	11.11
Invasive lobular carcinoma	1	1.11
Others	5	5.56

MRI, magnetic resonance imaging; SLU, second-look ultrasound; IDC, invasive ductal carcinoma.

ADC values than benign ones [ADC_{min}: (704.22±226.34)×10^{-6} *vs.* (894.95±291.91)×10^{-6} mm^2/s, P=0.001; ADC_{mean}: (894.45±181.73)×10^{-6} *vs.* (1,142.51±244.46)×10^{-6} mm^2/s, P<0.001; ADC_{max}: (1,051.12±281.70)×10^{-6} *vs.* (1,294.51±288.80)×10^{-6} mm^2/s, P<0.001]. Combining ADC_{min}, ADC_{mean}, and ADC_{max}, ROC analysis yielded AUC of 0.824, with sensitivity, specificity, PPV, and NPV of 78.43%, 79.49%, 0.833, and 0.738, respectively.

In masses, ADC_{mean} and ADC_{max} were significantly lower in the malignant group than in benign group [ADC_{mean}: (853.58±156.54)×10^{-6} *vs.* (1,113.19±257.64)×10^{-6} mm^2/s, P<0.001; ADC_{max}: (996.21±271.87)×10^{-6} *vs.* (1,247.14±246.41)×10^{-6} mm^2/s, P=0.002]. AUC obtained for differentiating benign from malignant MRI-only lesions was 0.833, with sensitivity, specificity, PPV, and NPV of 83.33%, 80.95%, 0.833, and 0.810, respectively.

In non-mass lesions, ADC_{min} [(745.89±208.38)×10^{-6} *vs.* (962.44±199.44)×10^{-6} mm^2/s, P=0.001] and ADC_{mean} [(930.78±197.29)×10^{-6} *vs.* (1,176.72±230.63)×10^{-6} mm^2/s, P<0.001] were significantly lower in malignant group than in benign group. For differentiating benign and malignant lesions, we obtained AUC of 0.815 (sensitivity, 74.07%; specificity, 83.33%; PPV, 0.870; NPV, 0.682).

$ADC_{heterogeneity}$ had no significant difference between benign and malignant tumors in all MRI-only lesions, masses, or non-mass lesions (P=0.43–0.62).

Added value of ADC parameters to BI-RADS parameters

For all lesions, the ADC parameters had an increased AUC compared to BI-RADS parameters (0.824 *vs.* 0.650, P=0.006 when the washout pattern was defined as malignant tumor; 0.824 *vs.* 0.673, P=0.006 when the washout or platform pattern was defined as malignant tumor). When the washout pattern was defined as malignant, the combination of significant BI-RADS and ADC parameters resulted in an AUC of 0.841 for differential diagnosis, with sensitivity, specificity, PPV, and NPV of 76.47%, 82.05%, 0.854, and 0.762, respectively. When the washout or platform pattern was defined as a malignant tumor, AUC obtained by combining significant BI-RADS and ADC parameters was 0.848 (sensitivity, 80.39%; specificity, 82.05%; PPV, 0.848; NPV, 0.727).

For non-mass lesions, combining significant BI-RADS and ADC parameters resulted in AUC, sensitivity, specificity, PPV and NPV of 0.862 (95% CI: 0.727, 0.947), 77.78%, 88.89%, 0.900, and 0.640, respectively.

ROC curves for all significant BI-RADS and ADC parameters are provided in Figure S1.

Discussion

Herein, we discriminated benign from malignant MRI-only suspicious lesions based on BI-RADS features and DWI characteristics. We investigated the additional value of ADC parameters which reflect $ADC_{heterogeneity}$ in the differential diagnosis of MRI-only lesions. Our findings showed that AUC of ADC parameters for diagnosing MRI-only lesions was higher than that of BI-RADS features. Conventional DWI acquisition may provide added value in differentiating MRI-only lesions. However, $ADC_{heterogeneity}$ has no significant additional value in our study.

BI-RADS features (qualitative morphological and kinetic features) contribute to lesion characterization in general clinical settings. However, for MRI-only lesions which are usually small, the value of morphological and kinetic features remains controversial in our clinical practice

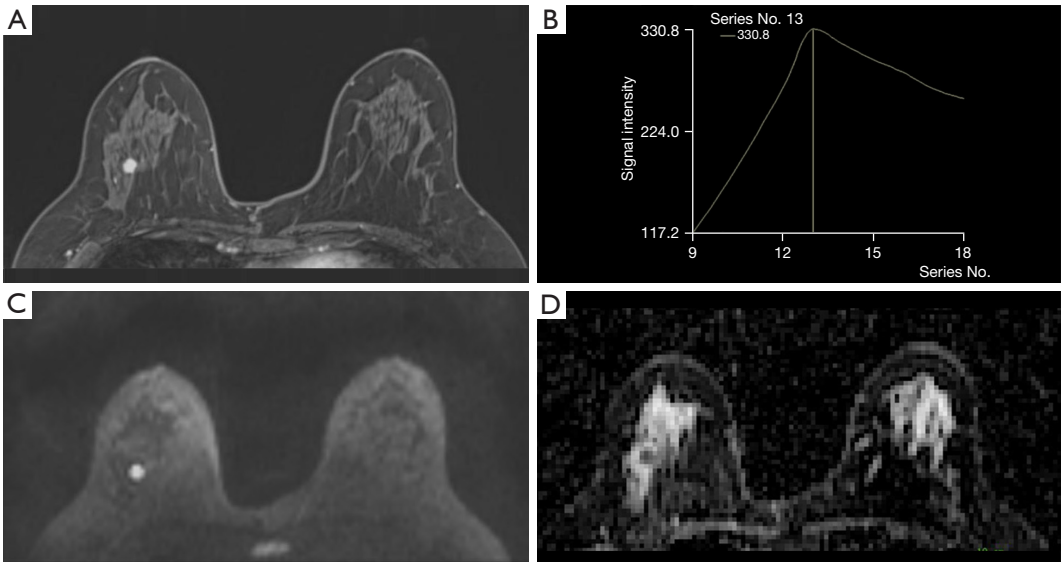

Figure 2 A 46-year-old patient with an MRI-only mass of 8 mm in the right breast. The contrast-enhanced T1-weighted image (A) showed the MRI-only lesion with oval shape, circumscribed margin and homogeneous enhancement. The kinetic curve showed a washout pattern with a peak of maximal signal intensity value of 330.8 about 1.5 minutes (B). On the DWI image (C) and ADC map (D), the minimum, maximum, and mean ADC values was 154.32×10^{-6}, 952.42×10^{-6}, and 752.33×10^{-6} mm^2/s, respectively. The histopathological diagnosis was IDC. The horizontal coordinates of (B) are the serial numbers of one pre-contrast and seven post-contrast images at 1-minute intervals. The curve was generated from series 9 (mask) and series 12–18 (post-contrast). Series 10–11 were post-processed images automatically generated by the scanning system and were skipped during the TIC generation. MRI, magnetic resonance imaging; DWI, diffusion weighted imaging; ADC, apparent diffusion coefficient; IDC, invasive ductal carcinoma.

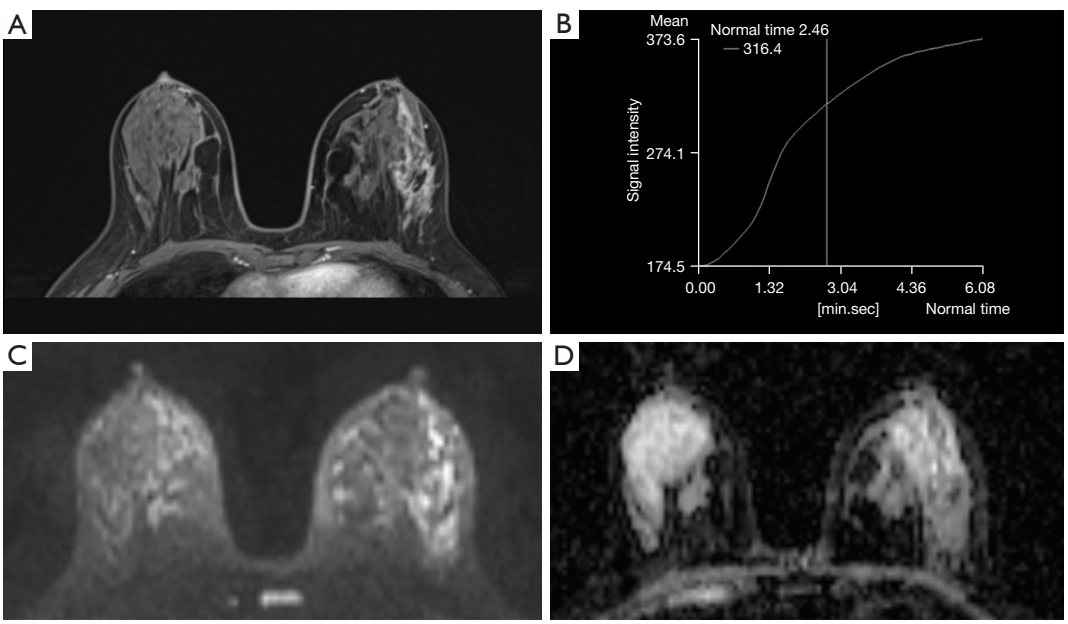

Figure 3 A 32-year-old patient with an MRI-only non-mass lesion in the left breast. On contrast-enhanced T1-weighted image (A), the non-mass lesion exhibited heterogeneous enhancement with a segmental distribution. The kinetic curve showed a persistent pattern (B). On the DWI image (C) and ADC map (D), the minimum, maximum, and mean ADC values was $1{,}173.25\times10^{-6}$, $1{,}241.36\times10^{-6}$, and $1{,}361.43\times10^{-6}$ mm^2/s, respectively. The histopathological diagnosis was plasma cell mastitis. The horizontal coordinate unit of (B) is minute. MRI, magnetic resonance imaging; DWI, diffusion weighted imaging; ADC, apparent diffusion coefficient.

Table 3 Comparison of BI-RADS parameters between benign and malignant MRI-only lesions

Variables	Overall	Malignant	Benign	P
Mass and non-mass	90	51	39	
Tumor size (mm)	17.5±16.4	19.6±17.8	14.8±14.2	0.16
Kinetic pattern 1				0.005
Persistent/plateau	47	20	27	
Washout	43	31	12	
Kinetic pattern 2				<0.001
Persistent	17	2	15	
Plateau/washout	73	49	24	
Mass	45	24	21	
Tumor size (mm)	7.4±2.1	7.5±2.4	7.4±1.7	0.85
Shape				0.34
Oval/round	30	14	16	
Irregular	15	10	5	
Margin				0.15
Circumscribed	10	3	7	
Not circumscribed	35	21	14	
Internal enhancement				0.07
Homogeneous	34	15	19	
Heterogeneous/rim enhancement	11	9	2	
Non-mass	45	27	18	
Tumor size (mm)	27.6±18.2	30.4±18.6	23.5±17.3	0.004
Distribution				<0.001
Focal	19	4	15	
Others	26	23	3	
Internal enhancement				0.12
Homogeneous/heterogeneous	16	7	9	
Others	29	20	9	

Data are mean ± standard deviation or frequency. Kinetic pattern 1 defined washout curve as malignancy; kinetic pattern 2 defined washout or plateau curve as malignancy. BI-RADS, Breast Imaging Reporting and Data System; MRI, magnetic resonance imaging.

experience. Therefore, on the one hand, we compared the performance of quantitative ADC parameters with qualitative morphological and kinetic features; on the other hand, we aimed to verify the value of morphological and kinetic features in MRI-only lesions. However, our study did not find any helpful BI-RADS-based morphological features for further discriminating MRI-only lesions. The two kinetic pattern criteria for differentiating MRI-only lesions produced moderate AUCs of 0.650 (95% CI: 0.542, 0.748) and 0.673 (95% CI: 0.566, 0.768), respectively. The above results demonstrated that the BI-RADS features are of limited value for further discriminating MRI-only lesions.

In the subgroup analysis, our findings revealed that

Table 4 Comparison of ADC parameters between benign and malignant MRI-only lesions

Morphology	Variables	Benign tumors	Malignant tumors	P*
Mass and non-mass	ADC_{min}	894.95±291.91	704.22±226.34	0.001
	ADC_{mean}	1,142.51±244.46	894.45±181.73	<0.001
	ADC_{max}	1,294.51±288.80	1,051.12±281.70	<0.001
	$ADC_{heterogeneity}$	2.12±3.24	1.83±1.95	0.59
Mass	ADC_{min}	837.10±347.10	657.33±240.72	0.05
	ADC_{mean}	1,113.19±257.64	853.58±156.54	<0.001
	ADC_{max}	1,247.14±246.41	996.21±271.87	0.002
	$ADC_{heterogeneity}$	2.71±4.36	2.18±2.81	0.62
Non-mass	ADC_{min}	962.44±199.44	745.89±208.38	0.001
	ADC_{mean}	1,176.72±230.63	930.78±197.29	<0.001
	ADC_{max}	1,349.78±330.14	1,099.93±286.34	0.01
	$ADC_{heterogeneity}$	1.43±0.34	1.52±0.36	0.43

Data are presented as mean ± standard deviation. The unit for ADC_{min}, ADC_{mean}, ADC_{max} is $\times 10^{-6}$ mm^2/s. *, adjusted P values ≤0.0042 were considered statistically significant. ADC, apparent diffusion coefficient; MRI, magnetic resonance imaging.

Table 5 AUC for differentiating benign and malignant MRI-only lesions

Morphology	Variables	AUC	95% CI	Sensitivity (%)	Specificity (%)
Mass and non-mass	Kinetic pattern 1	0.650	0.542, 0.748	60.78	69.23
	Kinetic pattern 2	0.673	0.566, 0.768	96.08	38.46
	ADC_{min}	0.746	0.643, 0.832	86.27	61.54
	ADC_{mean}	0.809	0.713, 0.884	70.59	84.62
	ADC_{max}	0.748	0.646, 0.834	56.86	87.18
	ADC_{min} + ADC_{mean} + ADC_{max}	0.824	0.729, 0.896	78.43	79.49
	ADC_{min} + ADC_{mean} + ADC_{max} + kinetic pattern 1	0.841	0.749, 0.910	76.47	82.05
	ADC_{min} + ADC_{mean} + ADC_{max} + kinetic pattern 2	0.848	0.757, 0.915	80.39	82.05
Mass	ADC_{mean}	0.825	0.683, 0.922	79.17	80.95
	ADC_{max}	0.794	0.647, 0.900	70.83	90.48
	ADC_{mean} + ADC_{max}	0.833	0.692, 0.928	83.33	80.95
Non-mass	Distribution	0.620	0.464, 0.761	74.07	50.00
	Mean tumor size	0.738	0.585, 0.857	70.37	77.78
	Distribution + mean tumor size	0.745	0.593, 0.863	62.96	88.89
	ADC_{min}	0.790	0.643, 0.897	81.48	72.22
	ADC_{mean}	0.812	0.667, 0.913	70.37	83.33
	ADC_{min} + ADC_{mean}	0.815	0.671, 0.915	74.07	83.33
	ADC_{min} + ADC_{mean} + distribution + mean tumor size	0.862	0.727, 0.947	77.78	88.89

Kinetic pattern 1 defined washout curve as malignancy; kinetic pattern 2 defined washout or plateau curve as malignancy. AUC, area under the ROC curve; ROC, receiver operating characteristic; MRI, magnetic resonance imaging; CI, confidence interval; ADC, apparent diffusion coefficient.

MRI-only masses had no pathognomonic BI-RADS features, and we noticed that these masses were small, almost none exceeding one centimeter. Diagnosing small masses is challenging, and our results are consistent with previous studies focusing on subcentimeter masses. For example, Xie *et al.* (17), in their analysis of qualitative and quantitative features of DCE-MRI in small masses, found that only kinetic patterns defining washout or plateau pattern as malignancy in DCE-MRI qualitative features could provide significant value for diagnosing small breast cancer. Similarly, Meissnitzer *et al.* (18) demonstrated that the morphological characteristics of small MRI lesions may be useless in differentiating benign from malignant lesions. For non-mass lesions, PPV of BI-RADS characteristics for lesion diagnosis varied significantly among studies, which may be related to factors such as subjectivity of readers and different disease types in various studies (19). In the present study, we showed that the distribution (e.g., segmental and linear) and size of non-mass lesions were proper BI-RADS features for differentiating MRI-only lesions. However, when combining the two parameters, the AUC was only 0.745 (95% CI: 0.593, 0.863).

DWI is the most valuable and robust adjunct to DCE, and their combination has high diagnostic sensitivity and specificity (16,20). It has also been pointed out that DWI with ADC maps can be used as a non-enhanced technique for breast cancer diagnosis and help reduce adverse events with contrast agents. This is consistent with our study that ADC parameters combined with BI-RADS features demonstrated higher diagnostic performance (AUC =0.841–0.848) for MRI-only lesions than DWI or BI-RADS parameters alone.

ADC values can quantitatively evaluate the diffusion restriction of water molecules in lesion tissues. Many studies confirmed the value of ADC in differentiating benign from malignant tumors (11,21). ADC_{mean} was higher in benign than in malignant lesions, which is consistent with our findings. Simultaneously, our study showed that ADC_{mean} had the highest diagnostic performance among all the significant ADC parameters (AUC =0.809–0.825), regardless of tumor type (mass or non-mass). This result is consistent with the finding of McDonald *et al.* (22), who concluded that ADC_{mean} is a simple and sufficient biomarker and is able to improve the diagnostic ability of breast MRI compared to complex ADC measurement methods. Recently, the value of ADC_{min} in diagnosing breast cancer has aroused the attention of some scholars (23-25). ADC_{min} values represent the highest cellular area composed of tumor stroma. They can reflect the most malignant area in malignant lesions, while ADC_{max} values represent the lowest cellular area and are susceptible to fibrosis and necrosis. Hirano *et al.* (26) found that ADC_{min} was the best ADC parameter to distinguish benign and malignant breast masses by evaluating the efficacy of ADC_{min}, ADC_{mean}, ADC_{max}, and ADC difference in the differential diagnosis of breast masses, and the diagnostic performance of ADC_{min} combined with ADC difference was superior to ADC_{mean}. This differs from our current findings in that ADC_{mean} in our study was still the best parameter in diagnosing breast masses. The discrepant results may be related to the small lesion size and less necrosis of masses in our study. In addition, it is related to the different ROI delineation methods. Hirano *et al.* (26) determined ADC_{min} by selecting the lowest value from multiple small ROIs. Our study selected the lowest value of pixels in large single-slice 2D ROIs, referring to previous study (16). Furthermore, we found that ADC_{min} performed only inferior to ADC_{mean} in the diagnosis of non-mass lesions, indicating that ADC_{min} can probably reflect the most aggressive component of non-mass lesions.

$ADC_{heterogeneity}$ represents a quantitative imaging biomarker of intratumoral heterogeneity, and few studies investigated the diagnostic ability of $ADC_{heterogeneity}$ for breast lesions. According to Zhuang *et al.* (27), ΔADC (i.e., $ADC_{max} - ADC_{min}$) was useful in predicting the proliferative status of Ki-67 in breast invasive ductal carcinomas (IDC) and had the highest AUC for assessing the Ki-67 labeling index. Additionally, Yoon *et al.* (28) demonstrated that a higher $ADC_{heterogeneity}$ was significantly associated with the invasive component of ductal carcinoma *in situ*. However, our current study fails to reflect the value of $ADC_{heterogeneity}$ in the differential diagnosis of MRI-only lesions. This may be due to the small size of MRI-only masses and their limited voxels. Meanwhile, non-mass lesions are mixed with adipose and glandular tissues which probably affect the evaluation of tumor heterogeneity. Additionally, the delineation of single-slice ROIs may not accurately reflect internal tumor heterogeneity.

There are several limitations of this study. First, this was a single-center retrospective study with a small number of patients and possible selection bias. Second, the International Breast DWI working group of the European Society of Breast Radiology (EUSOBI) (8) recommends the use of a small ROI in the darkest part of the lesion on the ADC map to improve inter-reader agreement, whereas in our study we used large 2D ROIs to delineate tumors

on ADC maps. This is because the MRI-only lesions in our sample were rather small, particularly the masses, whose average size was only 7.4 mm and in which necrosis was rarely observed. Therefore, rather than a small ROI corresponding to the darkest part, we employed a 2D ROI covering the whole lesion section in ADC measurements. Third, our DWI protocol used an in-plane resolution of 2.1×3.5 mm^2, which was greater than the upper limit of 2×2 mm^2 recommended by the International Breast DWI working group of the EUSOBI, and images with this resolution may lack the necessary texture or details required to effectively reflect heterogeneity. Fourth, the performance evaluation for multivariate analysis did not employ cross-validation in this study, and therefore the ROC analysis of the multivariate models might be overfitted. Fifth, six ipsilateral breast lesions were included in our study, which probably included homologous lesions. Finally, we used only four simple ADC parameters to investigate their diagnostic performance for MRI-only lesions. Whether texture parameters and radiomics are helpful for the differentiation of MRI-only lesions deserves further research.

Conclusions

DWI quantitative parameters may significantly improve diagnostic ability of BI-RADS-based features of breast MRI and provide additional value for the discrimination of MRI-only suspicious lesions. Furthermore, ADC_{mean} is the best ADC parameter for differential diagnosis of MRI-only suspicious lesions. However, no added diagnostic value for $ADC_{heterogeneity}$ was found in this study.

Acknowledgments

Funding: None.

Footnote

Reporting Checklist: The authors have completed the STARD reporting checklist. Available at https://qims.amegroups.com/article/view/10.21037/qims-23-331/rc

Conflicts of Interest: All authors have completed the ICMJE uniform disclosure form (available at https://qims.amegroups.com/article/view/10.21037/qims-23-331/coif). The authors have no conflicts of interest to declare.

Ethical Statement: The authors are accountable for all aspects of the work in ensuring that questions related to the accuracy or integrity of any part of the work are appropriately investigated and resolved. This retrospective study was conducted in accordance with the Declaration of Helsinki (as revised in 2013) and was approved by the Institutional Review Board of Beijing Hospital (No. 2022BJYYEC-388-01). The requirement for written informed consent was waived due to the retrospective nature of the study.

References

1. Mann RM, Cho N, Moy L. Breast MRI: State of the Art. Radiology 2019;292:520-36.
2. Eghtedari M, Chong A, Rakow-Penner R, Ojeda-Fournier H. Current Status and Future of BI-RADS in Multimodality Imaging, From the AJR Special Series on Radiology Reporting and Data Systems. AJR Am J Roentgenol 2021;216:860-73.
3. Kolta M, Clauser P, Kapetas P, Bernathova M, Pinker K, Helbich TH, Baltzer PAT. Can second-look ultrasound downgrade MRI-detected lesions? A retrospective study. Eur J Radiol 2020;127:108976.
4. Au FW, Ghai S, Lu FI, Lu H. Clinical Value of Shear Wave Elastography Added to Targeted Ultrasound (Second-Look Ultrasound) in the Evaluation of Breast Lesions Suspicious of Malignancy Detected on Magnetic Resonance Imaging. J Ultrasound Med 2019;38:2395-406.
5. Lee SH, Kim SM, Jang M, Yun BL, Kang E, Kim SW, Park SY, Ahn HS, Chang JH, Yoo Y, Song TK, Moon WK. Role of second-look ultrasound examinations for MR-detected lesions in patients with breast cancer. Ultraschall Med 2015;36:140-8.
6. Lambert J, Steelandt T, Heywang-Köbrunner SH, Gieraerts K, Van Den Berghe I, Van Ongeval C, Casselman JW. Long-term MRI-guided vacuum-assisted breast biopsy results of 600 single-center procedures. Eur Radiol 2021;31:4886-97.

7. Tang A, Cohan CM, Hansen KS, Beattie G, Greenwood HI, Mukhtar RA. Relationship between body mass index and malignancy rates of MRI-guided breast biopsies: impact of clinicodemographic factors. Breast Cancer Res Treat 2021;188:739-47.
8. Baltzer P, Mann RM, Iima M, Sigmund EE, Clauser P, Gilbert FJ, Martincich L, Partridge SC, Patterson A, Pinker K, Thibault F, Camps-Herrero J, Le Bihan D; . Diffusion-weighted imaging of the breast-a consensus and mission statement from the EUSOBI International Breast Diffusion-Weighted Imaging working group. Eur Radiol 2020;30:1436-50.
9. An Y, Mao G, Ao W, Mao F, Zhang H, Cheng Y, Yang G. Can DWI provide additional value to Kaiser score in evaluation of breast lesions. Eur Radiol 2022;32:5964-73.
10. Almutlaq ZM, Wilson DJ, Bacon SE, Sharma N, Stephens S, Dondo T, Buckley DL. Evaluation of Monoexponential, Stretched-Exponential and Intravoxel Incoherent Motion MRI Diffusion Models in Early Response Monitoring to Neoadjuvant Chemotherapy in Patients With Breast Cancer-A Preliminary Study. J Magn Reson Imaging 2022;56:1079-88.
11. Lee SA, Lee Y, Ryu HS, Jang MJ, Moon WK, Moon HG, Lee SH. Diffusion-weighted Breast MRI in Prediction of Upstaging in Women with Biopsy-proven Ductal Carcinoma in Situ. Radiology 2022;305:307-16.
12. Spick C, Pinker-Domenig K, Rudas M, Helbich TH, Baltzer PA. MRI-only lesions: application of diffusion-weighted imaging obviates unnecessary MR-guided breast biopsies. Eur Radiol 2014;24:1204-10.
13. Amornsiripanitch N, Rahbar H, Kitsch AE, Lam DL, Weitzel B, Partridge SC. Visibility of mammographically occult breast cancer on diffusion-weighted MRI versus ultrasound. Clin Imaging 2018;49:37-43.
14. Xu M, Tang Q, Li M, Liu Y, Li F. An analysis of Ki-67 expression in stage 1 invasive ductal breast carcinoma using apparent diffusion coefficient histograms. Quant Imaging Med Surg 2021;11:1518-31.
15. Jeong S, Kim TH. Diffusion-weighted imaging of breast invasive lobular carcinoma: comparison with invasive carcinoma of no special type using a histogram analysis. Quant Imaging Med Surg 2022;12:95-105.
16. Kim JJ, Kim JY, Suh HB, Hwangbo L, Lee NK, Kim S, Lee JW, Choo KS, Nam KJ, Kang T, Park H. Characterization of breast cancer subtypes based on quantitative assessment of intratumoral heterogeneity using dynamic contrast-enhanced and diffusion-weighted magnetic resonance imaging. Eur Radiol 2022;32:822-33.
17. Xie T, Zhao Q, Fu C, Bai Q, Zhou X, Li L, Grimm R, Liu L, Gu Y, Peng W. Differentiation of triple-negative breast cancer from other subtypes through whole-tumor histogram analysis on multiparametric MR imaging. Eur Radiol 2019;29:2535-44.
18. Meissnitzer M, Dershaw DD, Feigin K, Bernard-Davila B, Barra F, Morris EA. MRI appearance of invasive subcentimetre breast carcinoma: benign characteristics are common. Br J Radiol 2017;90:20170102.
19. Lunkiewicz M, Forte S, Freiwald B, Singer G, Leo C, Kubik-Huch RA. Interobserver variability and likelihood of malignancy for fifth edition BI-RADS MRI descriptors in non-mass breast lesions. Eur Radiol 2020;30:77-86.
20. Marino MA, Avendano D, Sevilimedu V, Thakur S, Martinez D, Lo Gullo R, Horvat JV, Helbich TH, Baltzer PAT, Pinker K. Limited value of multiparametric MRI with dynamic contrast-enhanced and diffusion-weighted imaging in non-mass enhancing breast tumors. Eur J Radiol 2022;156:110523.
21. Lo Gullo R, Sevilimedu V, Baltzer P, Le Bihan D, Camps-Herrero J, Clauser P, Gilbert FJ, Iima M, Mann RM, Partridge SC, Patterson A, Sigmund EE, Thakur S, Thibault FE, Martincich L, Pinker K; EUSOBI International Breast Diffusion-Weighted Imaging Working Group. A survey by the European Society of Breast Imaging on the implementation of breast diffusion-weighted imaging in clinical practice. Eur Radiol 2022;32:6588-97.
22. McDonald ES, Romanoff J, Rahbar H, Kitsch AE, Harvey SM, Whisenant JG, et al. Mean Apparent Diffusion Coefficient Is a Sufficient Conventional Diffusion-weighted MRI Metric to Improve Breast MRI Diagnostic Performance: Results from the ECOG-ACRIN Cancer Research Group A6702 Diffusion Imaging Trial. Radiology 2021;298:60-70.
23. Li T, Hong Y, Kong D, Li K. Histogram analysis of diffusion kurtosis imaging based on whole-volume images of breast lesions. J Magn Reson Imaging 2020;51:627-34.
24. Ulu E, Ozturk B, Atalay K, Okumus IB, Erdem D, Gul MK, Terzi O. Diffusion-Weighted Imaging of Brain Metastasis: Correlation of MRI Parameters with Histologic Type. Turk Neurosurg 2022;32:58-68.
25. Fang J, Zhang Y, Li R, Liang L, Yu J, Hu Z, Zhou L, Liu R. The utility of diffusion-weighted imaging for differentiation of phyllodes tumor from fibroadenoma and breast cancer. Front Oncol 2023;13:938189.
26. Hirano M, Satake H, Ishigaki S, Ikeda M, Kawai H, Naganawa S. Diffusion-weighted imaging of breast

masses: comparison of diagnostic performance using various apparent diffusion coefficient parameters. AJR Am J Roentgenol 2012;198:717-22.
27. Zhuang Z, Zhang Q, Zhang D, Cheng F, Suo S, Geng X, Hua J, Xu J. Utility of apparent diffusion coefficient as an imaging biomarker for assessing the proliferative potential of invasive ductal breast cancer. Clin Radiol 2018;73:473-8.
28. Yoon HJ, Kim Y, Kim BS. Intratumoral metabolic heterogeneity predicts invasive components in breast ductal carcinoma in situ. Eur Radiol 2015;25:3648-58.

Cite this article as: Li X, Wang H, Gao J, Jiang L, Chen M. Quantitative apparent diffusion coefficient metrics for MRI-only suspicious breast lesions: any added clinical value? Quant Imaging Med Surg 2023;13(10):7092-7104. doi: 10.21037/qims-23-331

